
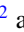






Coherent phonons and the interplay between charge density wave and Mott phases in 1T-TaSe₂C. J. Sayers ^{1,2,*}, H. Hedayat,^{1,3} A. Ceraso,¹ F. Museur,⁴ M. Cattelan ⁵, L. S. Hart,² L. S. Farrar ², S. Dal Conte,¹ G. Cerullo ¹, C. Dallera,¹ E. Da Como ² and E. Carpene ³¹*Dipartimento di Fisica, Politecnico di Milano, 20133 Milano, Italy*²*Centre for Nanoscience and Nanotechnology, Department of Physics, University of Bath, Bath, BA2 7AY, United Kingdom*³*IFN-CNR, Dipartimento di Fisica, Politecnico di Milano, 20133 Milano, Italy*⁴*Université de Lyon, ENS de Lyon, Université Claude Bernard, CNRS, Laboratoire de Physique, F-69342 Lyon, France*⁵*School of Chemistry, University of Bristol, Cantocks Close, Bristol BS8 ITS, United Kingdom*

(Received 16 July 2020; revised 4 September 2020; accepted 9 September 2020; published 8 October 2020)

1T-TaSe₂ is host to coexisting strongly correlated phases including charge density waves (CDWs) and an unusual Mott transition at low temperature. Here, we investigate coherent phonon oscillations in 1T-TaSe₂ using a combination of time- and angle-resolved photoemission spectroscopy (TR-ARPES) and time-resolved reflectivity (TRR). Perturbation by a femtosecond laser pulse triggers a modulation of the valence band binding energy at the $\bar{\Gamma}$ point, related to the Mott gap, that is consistent with the in-plane CDW amplitude mode frequency. By contrast, TRR measurements show a modulation of the differential reflectivity comprised of multiple frequencies belonging to the distorted CDW lattice modes. Comparison of the temperature dependence of coherent and spontaneous phonons across the CDW transition shows that the amplitude mode intensity is more easily suppressed during perturbation of the CDW state by the optical excitation compared to other modes. Our results clearly identify the relationship of the in-plane CDW amplitude mode with the Mott phase in 1T-TaSe₂ and highlight the importance of lattice degrees of freedom.

DOI: [10.1103/PhysRevB.102.161105](https://doi.org/10.1103/PhysRevB.102.161105)**I. INTRODUCTION**

Understanding the delicate interplay between co-operating or competing phases of matter in quantum materials is an ongoing goal of fundamental research [1–3]. Driving these systems out of equilibrium using an intense femtosecond laser pulse offers the possibility to transiently suppress forms of electronic and lattice order and monitor their recovery in real time [4]. The characteristic dynamics of these processes allows a classification of materials in the time domain [5], and has been used to disentangle the underlying mechanisms of complex phases found in cuprate superconductors [6] and exciton-lattice-driven charge density wave (CDW) systems [7], or to unlock normally hidden states of matter [8].

An ideal platform to investigate these phenomena are the trigonal (1T) tantalum-based transition metal dichalcogenides, MX₂ ($M = \text{Ta}$, $X = \text{S/Se}$) which are host to a whole range of strongly correlated behavior including CDWs [9], Mott physics [10], possible quantum spin liquid states [11], and superconductivity [12,13].

Tantalum disulphide (1T-TaS₂) has been studied extensively using time-resolved techniques [14–20], motivated mostly by its rich phase diagram. It exhibits multiple CDW transitions including an incommensurate (550 K), nearly commensurate (350 K), and commensurate (180 K) phase [9] that occurs concomitantly with a metal-insulator transition, commonly associated with a Mott phase [21]. However, an

alternative explanation has recently been proposed based on the three-dimensional stacking order of the CDW and hybridization of atomic orbitals [22–24]. Thus, important questions surrounding the nature of the metal-insulator transition and its relationship with the CDW remain.

Tantalum diselenide (1T-TaSe₂) has received comparatively far less attention, although it was recently suggested to be the more suitable compound to investigate the relationship between the CDW and Mott phases because of the well-separated transition temperatures, larger electronic gap, and reduced complexity due to the absence of the nearly commensurate phase [19].

1T-TaSe₂ undergoes a first-order transition from an incommensurate (ICCDW) to commensurate (CCDW) charge density wave at $T_{\text{CDW}} = 473$ K [25]. It is accompanied by an in-plane $\sqrt{13}a_0 \times \sqrt{13}a_0$ periodic lattice distortion (PLD) which is rotated by $\sim 13^\circ$ with respect to the original unit cell, and forms a 13-atom superlattice comprised of Ta clusters in the so-called “star-of-David” configuration [9].

In addition to the well-known CDW, a Mott transition occurs at ~ 260 K evidenced by the opening of a gap, $\Delta_{\text{Mott}} \approx 250$ meV below the Fermi level, E_{F} , observed by ARPES [10] and STM [26]. The CDW has been suggested to be a precursor to the Mott phase, since it modifies the band structure resulting in a narrow half-filled band at E_{F} . As the temperature is reduced, the increasing CDW amplitude causes a narrowing of the bandwidth (W), related to the in-plane electron hopping between the adjacent star-of-David clusters in the CDW lattice [27,28]. Electrons will become localized when the bandwidth (W) decreases below a critical value

*Corresponding author: charles.sayers@polimi.it

and the Mott criterion $U/W \geq 1$ is reached, where U is the on-site electron-electron Coulomb repulsion. The result of this localization is a transition to an insulating state and formation of a gap, Δ_{Mott} [10,26].

Time- and angle-resolved photoemission spectroscopy (TR-ARPES) is a powerful tool which allows direct visualization of the electronic band structure following perturbation with a laser pulse. In strongly correlated systems, it can be used to monitor the collapse and recovery of electronic order in real time by probing energy gaps Δ related to the order parameter [5–7]. Recent TR-ARPES studies of 1T-TaSe₂ using high harmonics ($h\nu \approx 22$ eV) have focused predominantly on gap suppression dynamics on short timescales [19] or the room temperature (CDW) phase only [29], and thus the Mott phase dynamics remain relatively unexplored.

Here, we report on electron and phonon dynamics of 1T-TaSe₂ at low temperature (77 K) where the CDW and Mott phases coexist. Using TR-ARPES with $h\nu = 6$ eV photon energy, we track the temporal evolution of the valence band binding energy related to Δ_{Mott} at the $\bar{\Gamma}$ point over several picoseconds. We find that it exhibits strong, long-lasting oscillations with a single frequency related to the in-plane CDW amplitude mode (~ 2.2 THz at 77 K). Using complementary time-resolved reflectivity (TRR) measurements, we instead find multiple phonon frequencies related to the PLD ($\sim 1.8, 2.2,$ and 2.9 THz). Therefore, aided by the momentum selectivity of TR-ARPES, our results reveal that the gap, Δ_{Mott} , is linked preferentially to the amplitude mode of the CDW. By investigating the temperature dependence of coherent phonons, we find that the amplitude mode deviates significantly from first-order behavior, while the other modes are robust up to T_{CDW} , highlighting further the nature of this mode and its importance to electronic order in this material.

II. METHODS

TR-ARPES experiments were performed using visible (~ 1.8 eV, 30 fs) pump and deep-ultraviolet (~ 6.0 eV, 80 fs) probe pulses generated by a series of nonlinear optical processes from the output of an Yb-based laser (Pharos, Light Conversion) operating at 80 kHz repetition rate, as described in Ref. [30]. The overall time and energy resolution of this configuration were approximately 80 fs and 45 meV, respectively. TRR was performed using a setup based on a Ti:sapphire laser (Coherent Libra) which drives two noncollinear parametric amplifiers serving as pump and probe beams [31]. The amplified pulses are characterized by a broad spectrum of (1.8–2.4) eV and compressed to ≤ 20 fs duration using chirped mirrors. Steady-state ARPES measurements were performed at the Bristol NanoESCA facility using He-I α radiation ($h\nu = 21.2$ eV), with ~ 50 meV energy resolution at 40 K. Further experimental details relating to crystal growth methods, electrical transport measurements, and Raman spectroscopy are provided in the Supplemental Material (Ref. [32]).

III. RESULTS AND DISCUSSION

First we discuss the electronic structure of 1T-TaSe₂ and the effects of CDW and Mott transitions. Figure 1(a) shows a

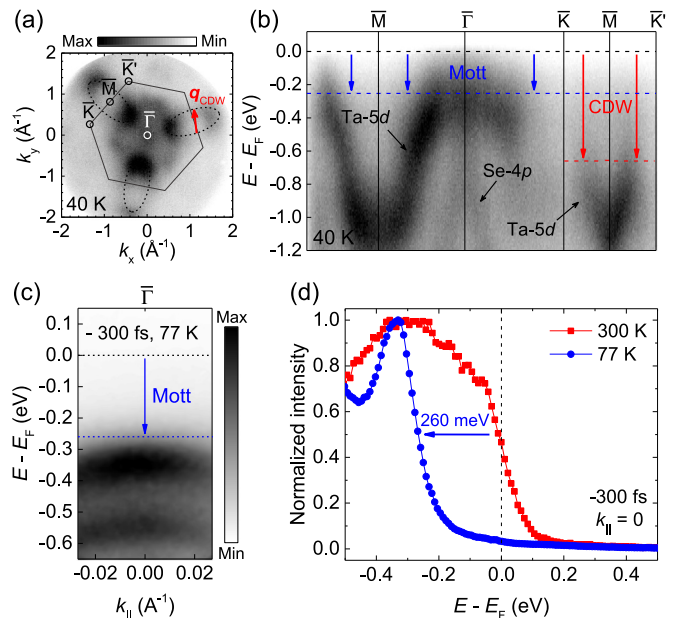


FIG. 1. Electronic order in 1T-TaSe₂. (a) Full-wave-vector ARPES ($h\nu = 21.2$ eV) image of the electronic structure, $E - E_F = -0.5$ eV at 40 K with projected high-symmetry points of the hexagonal Brillouin zone (BZ) labeled. The red arrow is the expected CDW vector, \mathbf{q}_{CDW} . (b) Band dispersions through the BZ. The vertical arrows highlight the lowering of occupied states due to the CDW (red) and Mott (blue) transitions. (c) TR-ARPES ($h\nu = 6$ eV) map at 77 K. (d) Comparison of EDCs extracted from the $\bar{\Gamma}$ point ($k_{\parallel} = 0$) at 300 and 77 K. The arrow shows the band edge shift as a result of the Mott transition.

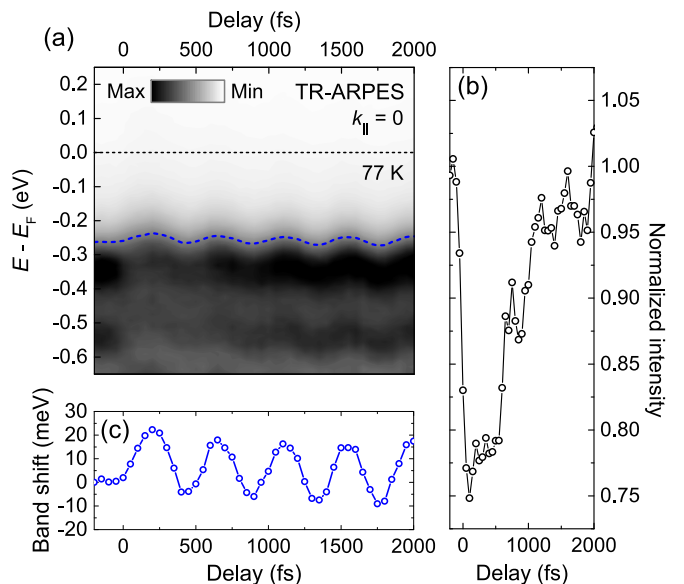


FIG. 2. Valence band dynamics in the CDW-Mott phase. (a) TR-ARPES spectra at the $\bar{\Gamma}$ point (77 K) using 1.10 mJ cm^{-2} pump fluence. (b) Normalized valence band intensity, extracted from the maximum near $E - E_F \approx -0.35$ eV. (c) Valence band shift extracted from a constant intensity contour in panel (a), indicated by the blue dashed line.

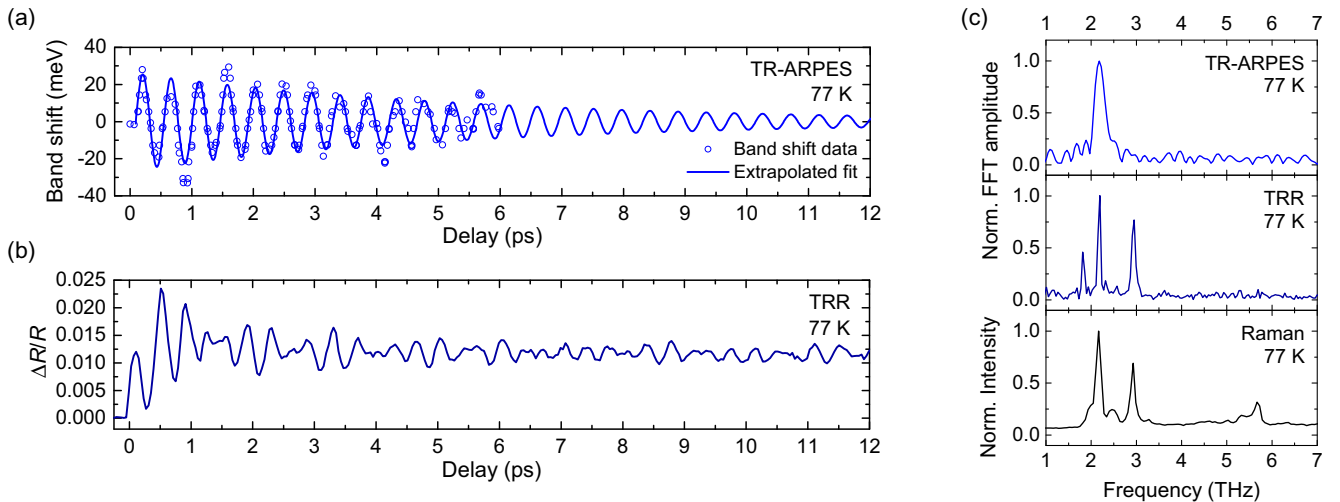


FIG. 3. Coherent phonon oscillations in the CDW-Mott phase. (a) Oscillatory component of the valence band shift measured by TR-ARPES (1.16 mJ cm^{-2}). (b) Transient reflectivity signal measured by TRR (0.11 mJ cm^{-2}), where $\Delta R/R$ is the absolute value of the differential reflectivity. The selected data is for 1.84 eV probe photon energy. (c) Normalized fast Fourier transform (FFT) amplitude of the TR-ARPES and TRR oscillatory components, together with a Raman spectrum for comparison.

full-wave-vector ARPES image at $E - E_F = -0.5 \text{ eV}$ where all the main features are visible. Centered around the \bar{M} points on the BZ boundary are the elliptical Ta-5d electron pockets, and at the BZ center ($\bar{\Gamma}$ point) is the Se-4p pocket, in agreement with previous ARPES measurements [33,34]. The CDW involves finite portions of the Ta-5d electron pockets which are linked by the wave vector \mathbf{q}_{CDW} in the $\bar{K}-\bar{M}-\bar{K}$ direction where the Fermi surface could be prone to nesting [9,19], although the importance of such electronic instabilities is still debated [33,35]. Indeed, there is a clear loss of intensity on the parallel arms of these pockets in Fig. 1(a), and dispersion along the $\bar{K}-\bar{M}-\bar{K}$ direction in Fig. 1(b) shows the band edge is found significantly below E_F as a result of the CDW gap, Δ_{CDW} . Dispersion along the $\bar{M}-\bar{\Gamma}$ direction in Fig. 1(b) shows a valence band comprised of broad Ta-5d states, and steeply dispersing Se-4p states, which are known to extend to E_F at room temperature [10]. At 40 K, all bands near E_F have been lowered by $\sim 250 \text{ meV}$ due to a gap Δ_{Mott} which extends across all k space, and thus the entire Fermi surface is removed [32].

Shown in Fig. 1(c) are TR-ARPES spectra of $1T\text{-TaSe}_2$ at 77 K near the $\bar{\Gamma}$ point before pump arrival (-300 fs). The dispersion is approximately along the $\bar{M}-\bar{\Gamma}-\bar{M}$ direction based on low-energy electron diffraction (LEED) [32]. Figure 1(c) clearly shows the band edge is situated below E_F due to the opening of a gap. A comparison of the energy distribution curves (EDCs) in Fig. 1(d) extracted at $\bar{\Gamma}$ ($k_{\parallel} = 0$) shows a lowering of the band edge by $\sim 260 \text{ meV}$ between 300 and 77 K, which is in very close agreement with previous reports of the Mott transition in $1T\text{-TaSe}_2$ [10] and the ARPES measurements in Fig. 1(b).

We note that such a substantial modification of the Fermi surface, as seen in Figs. 1(c) and 1(d), typically indicates the development of an insulating state, which would be expected to be observed by electrical transport [36]. However, our resistance measurements show metallic behavior to 4 K [32]. These contrasting results between surface probe (ARPES) and

bulk probe (transport) have previously provided support for the hypothesis that the Mott transition in $1T\text{-TaSe}_2$ is a surface effect [10]. However, we emphasize that for TR-ARPES at $h\nu = 6 \text{ eV}$, the inelastic mean free path for electrons is expected to be of the order $\sim 10 \text{ nm}$ [37] and hence the photoemission signal may represent several layers of $1T\text{-TaSe}_2$ given the c -axis length of 0.63 nm [25]. Thus, the Mott phase may extend over more than the surface layer.

We now focus on the valence band dynamics in the coexisting CDW-Mott phase measured by TR-ARPES. Figure 2(a) shows the valence band at the $\bar{\Gamma}$ point after perturbation by the pump pulse. At $t = 0$, the optical excitation results in an instantaneous loss of valence band intensity as highlighted in Fig. 2(b), and recovery occurs within $\sim 2 \text{ ps}$, which is similar to the reported dynamics of $1T\text{-TaS}_2$ in the Mott phase [14]. As is clearly evident by the persisting gap Δ_{Mott} in Fig. 2(a), we do not observe a collapse of the Mott phase and we also note that 1.10 mJ cm^{-2} pump fluence is not sufficient to melt the CDW [38]. Hence, we confirm that the TR-ARPES experiments were performed in the coexisting CDW-Mott phase.

Figure 2(c) shows the temporal evolution of the valence band edge position. Most noticeably, the pump triggers strong coherent oscillations which are weakly damped. TR-ARPES data in Fig. 3(a) shows a maximum initial oscillation of approximately $\pm 20 \text{ meV}$ around the equilibrium position with a large amplitude that persists at 6 ps. Fitting the data with a damped periodic function $E(t) = A \exp(-t/\tau_d) \sin(2\pi\omega t + \phi)$ yields a frequency $\omega \approx (2.19 \pm 0.01) \text{ THz}$, which closely matches the intense 72.4 cm^{-1} (2.17 THz) A_{1g} mode measured by Raman spectroscopy at 77 K [32]. The damping time was found to be $\tau_d \approx (6.3 \pm 1.0) \text{ ps}$. Such long-lived oscillations have also been observed in the Mott phase of $1T\text{-TaS}_2$ [14,15] and were assigned to the CDW amplitude mode, related to the in-plane breathing mode of the stars-of-David [39]. The result presented here shows a direct modulation of the binding energy of the valence band edge, related to Δ_{Mott} , by the CDW amplitude

mode in $1T$ -TaSe₂. This is consistent with the CDW precursor scenario whereby the CDW amplitude, related to the magnitude of the in-plane PLD, controls the U/W criterion by the degree of electron hopping between the adjacent stars-of-David [19,21,26–28]. By triggering coherent oscillations of the CDW amplitude (breathing) mode, we induce a modulation in the U/W ratio which manifests in the magnitude of Δ_{Mott} .

To investigate the origin of the coherent phonon oscillations further, we now compare our TR-ARPES results with TRR measurements. Figure 3(b) shows the temporal evolution of the differential reflectivity $\Delta R/R$ of $1T$ -TaSe₂ at 77 K. The $\Delta R/R$ signal is dominated by strong oscillations that are weakly damped and last up to 20 ps. Interestingly, the oscillations in TRR are comprised of multiple frequencies, in stark contrast to the single-frequency valence band modulation observed by TR-ARPES. This is confirmed by the fast Fourier transform (FFT) of the oscillatory components shown in Fig. 3(c). The FFT of the valence band dynamics shows a single frequency at ~ 2.2 THz, whereas FFT of the TRR signal shows multiple frequencies with greatest amplitude at ~ 1.8 , 2.2, and 2.9 THz, and closely resembles the Raman spectrum presented in Fig. 3(c) and reported previously [40–43]. We note that the ~ 1.8 THz mode cannot be seen in the Raman data as it falls below the cutoff of the spectrometer laser filter. In addition, we note that the 2.2 THz mode appears broader in the FFT of the TR-ARPES data because of the shorter sampling interval of the oscillations. Since both TR-ARPES and TRR experiments utilize comparable pump photon energies and pulse durations, it is conceivable that multiple modes are triggered in both cases and relate to the Raman-active Γ -point phonons of the PLD. The energy-momentum selectivity of TR-ARPES directly probes the local electronic structure of the valence band at Γ and the interactions there. Hence, the observed modulation of the valence band binding energy (Δ_{Mott}) with a single frequency belonging to the ~ 2.2 THz CDW amplitude mode, shows that the Mott phase is preferentially linked to that particular mode.

Having established the coherent phonon oscillations of the CDW lattice and the single mode which is linked to the Mott phase, we finally focus on the temperature dependence of these modes, and their behavior across the CDW transition at T_{CDW} . For this, we compare the response of the coherent phonons to optical excitation by TRR, and the spontaneous phonons of the PLD in quasiequilibrium by Raman spectroscopy. Shown in Fig. 4(a) is a FFT analysis of the $\Delta R/R$ signal for various sample temperatures in the range 295–478 K which are compared to Raman spectra in Fig. 4(b). Similar to the TRR data at 77 K, multiple frequency components are found at 295 K as shown in Fig. 4(a). The peaks in FFT amplitude belong to the two highest intensity modes determined previously [see Fig. 3(c)], although they are found at slightly lower frequencies of ~ 2.0 and 2.7 THz because of the higher sample temperature [32]. Figure 4(a) shows that as the temperature increases in the range 295–410 K, the intensity of the ~ 2.0 THz amplitude mode decreases sharply until it becomes undetectable for $T \geq 450$ K using 0.11 mJ cm^{-2} fluence. Instead, the ~ 2.7 THz mode remains present until heating above the first-order ICCDW-CCDW phase transition at $T_{\text{CDW}} = 473$ K. By comparison, the Raman

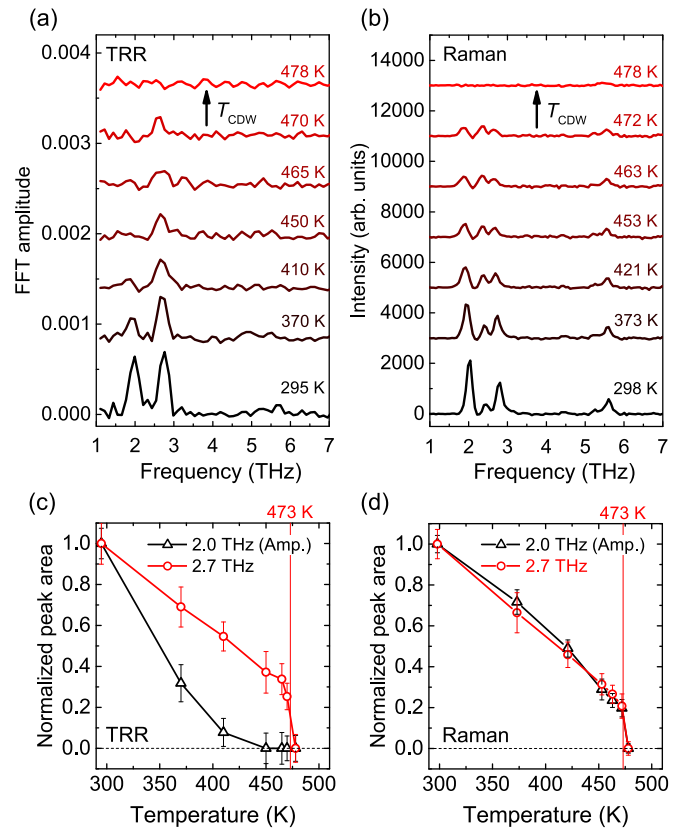


FIG. 4. Temperature dependence of coherent and spontaneous phonons in the CDW phase. (a) Fast Fourier transform (FFT) of the transient reflectivity $\Delta R/R$ signal measured by TRR (0.11 mJ cm^{-2}) at sample temperatures as indicated. The selected data is for 1.89 eV probe photon energy. (b) Raman spectra measured over a similar temperature range as panel (a) for comparison, after subtraction of a fit to the incoherent background signal above T_{CDW} (478 K). All traces are offset for clarity. Panels (c) and (d) show the temperature dependence of the integrated peak area for the 2.0 amplitude (Amp.) and 2.7 THz modes in the TRR-FFT and Raman spectra, respectively.

data in Fig. 4(b) shows that all modes remain clearly visible until there is a sudden change in the spectra when heating above T_{CDW} . Specifically, we find that all modes merge into a broad background (see Ref. [32]), similar to previous reports [40–43]. The stark difference in the temperature dependence of the mode intensities measured by the two experimental techniques is highlighted by comparing Figs. 4(c) and 4(d) which show the integrated peak areas in TRR and Raman spectroscopy, respectively. The expected first-order nature of the CDW transition is clear in Fig. 4(d) whereby there is a steep onset at T_{CDW} followed by linear temperature dependence, and both the ~ 2.0 and 2.7 THz modes exhibit identical behavior. Instead, Fig. 4(c) shows a dramatic suppression of the ~ 2.0 THz amplitude mode intensity and a deviation from first-order behavior in TRR, suggestive of a transient photoinduced melting of the CDW amplitude. The ~ 2.7 THz mode, however, which is a phonon of the PLD [41], appears to remain robust up to T_{CDW} . A complete loss of intensity of the CDW amplitude mode suggests that it has become strongly damped, whereby its lifetime is less than the period of oscillation (≈ 0.5 ps). Such increased damping could be

due to a reduced commensurability between the CDW and the underlying lattice which results in a faster dephasing of the oscillations [15], providing evidence for a suppression of the commensurate state by the optical excitation before the ICCDW-CCDW transition at T_{CDW} .

IV. CONCLUSION

In summary, an investigation of electron and phonon dynamics in the coexisting CDW-Mott phase of $1T$ -TaSe₂ using complementary TR-ARPES and TRR techniques clearly shows that the Mott phase is preferentially linked to the in-plane CDW amplitude, since it controls the degree of electron localization between adjacent star-of-David configurations.

Our results highlight the role of the CDW and lattice degrees of freedom in stabilizing the Mott phase of $1T$ -TaSe₂ and further the understanding of the interplay between these coexisting phases.

ACKNOWLEDGMENTS

The authors acknowledge funding and support from the EPSRC Centre for Doctoral Training in Condensed Matter Physics (CDT-CMP) Grant No. EP/L015544/1 and the Italian PRIN Project No. 2017BZPKSZ. We acknowledge the School of Chemistry at the University of Bristol for access to the Bristol NanoESCA Facility. Finally, we thank D. Wolverson for useful discussions.

-
- [1] L. J. Li, E. C. T. O'Farrell, K. P. Loh, G. Eda, B. Ozyilmaz, and A. H. C. Neto, Controlling many-body states by the electric field effect in a two-dimensional material, *Nature (London)* **529**, 185 (2016).
- [2] H. H. da Silva Neto, P. Aynajian, A. Frano, R. Comin, E. Schierle, E. Weschke, A. Gyenis, J. Wen, J. Schneeloch, Z. Xu, S. Ono, G. Gu, M. Le Tacon, and Mathieu A. Yazdani, Ubiquitous interplay between charge ordering and high-temperature superconductivity in cuprates, *Science* **343**, 393 (2014).
- [3] A. Kogar, G. A. de la Pena, Sangjun Lee, Y. Fang, S. X. L. Sun, D. B. Lioi, G. Karapetrov, K. D. Finkelstein, J. P. C. Ruff, P. Abbamonte, and S. Rosenkranz, Observation of a Charge Density Wave Incommensuration Near the Superconducting Dome in Cu_xTiSe₂, *Phys. Rev. Lett.* **118**, 027002 (2017).
- [4] C. Giannetti, M. Capone, D. Fausti, M. Fabrizio, F. Parmigiani, and D. Mihailovic, Ultrafast optical spectroscopy of strongly correlated materials and high-temperature superconductors: A non-equilibrium approach, *Adv. Phys.* **65**, 58 (2016).
- [5] S. Hellmann, T. Rohwer, M. Kalläne, K. Hanff, C. Sohrt, A. Stange, A. Carr, M. M. Murnane, H. C. Kapteyn, L. Kipp, M. Bauer, and K. Rossnagel, Time-domain classification of charge-density-wave insulators, *Nat. Commun.* **3**, 1069 (2012).
- [6] F. Boschini, E. H. da Silva Neto, E. Razzoli, M. Zonno, S. Peli, R. P. Day, M. Michiardi, M. Schneider, B. Zwartsenberg, P. Nigge, R. D. Zhong, J. Schneeloch, G. D. Gu, S. Zhdanovich, A. K. Mills, G. Levy, D. J. Jones, C. Giannetti and A. Damascelli, Collapse of superconductivity in cuprates via ultrafast quenching of phase coherence, *Nat. Mater.* **17**, 416 (2018).
- [7] H. Hedayat, C. J. Sayers, D. Bugini, C. Dallera, D. Wolverson, T. Batten, S. Karbassi, S. Friedemann, G. Cerullo, J. van Wezel, S. R. Clark, E. Carpena, and E. Da Como, Excitonic and lattice contributions to the charge density wave in $1T$ -TiSe₂ revealed by a phonon bottleneck, *Phys. Rev. Research* **1**, 023029 (2019).
- [8] K. Sun, S. Sun, C. Zhu, H. Tian, H. Yang, and J. Li, Hidden CDW states and insulator-to-metal transition after a pulsed femtosecond laser excitation in layered chalcogenide $1T$ -TaS_{2-x}Se_x, *Sci. Adv.* **4**, eaas9660 (2018).
- [9] J. A. Wilson, F. J. Di Salvo, and S. Mahajan, Charge-density waves and superlattices in the metallic layered transition metal dichalcogenides, *Adv. Phys.* **24**, 117 (1975).
- [10] L. Perfetti, A. Georges, S. Florens, S. Biermann, S. Mitrovic, H. Berger, Y. Tomm, H. Höchst, and M. Grioni, Spectroscopic Signatures of a Bandwidth-Controlled Mott Transition at the Surface of $1T$ -TaSe₂, *Phys. Rev. Lett.* **90**, 166401 (2003).
- [11] K. T. Law and P. A. Lee, $1T$ -TaS₂ as a quantum spin liquid, *Proc. Natl. Acad. Sci. USA* **114**, 6996 (2017).
- [12] B. Sipos, A. F. Kusmartseva, A. Akrap, H. Berger, L. Forró and E. Tutiš, From Mott state to superconductivity in $1T$ -TaS₂, *Nat. Mater.* **7**, 960 (2008).
- [13] Y. Liu, D. F. Shao, L. J. Li, W. J. Lu, X. D. Zhu, P. Tong, R. C. Xiao, L. S. Ling, C. Y. Xi, L. Pi, H. F. Tian, H. X. Yang, J. Q. Li, W. H. Song, X. B. Zhu, and Y. P. Sun, Nature of charge density waves and superconductivity in $1T$ -TaSe_{2-x}Te_x, *Phys. Rev. B* **94**, 045131 (2016).
- [14] L. Perfetti, P. A. Loukakos, M. Lisowski, U. Bovensiepen, H. Berger, S. Biermann, P. S. Cornaglia, A. Georges, and M. Wolf, Time Evolution of the Electronic Structure of $1T$ -TaS₂ through the Insulator-Metal Transition, *Phys. Rev. Lett.* **97**, 067402 (2006).
- [15] L. Perfetti, P. A. Loukakos, M. Lisowski, U. Bovensiepen, M. Wolf, H. Berger, S. Biermann and A. Georges, Femtosecond dynamics of electronic states in the Mott insulator $1T$ -TaS₂ by time resolved photoelectron spectroscopy, *New J. Phys.* **10**, 053019 (2008).
- [16] J. C. Petersen, S. Kaiser, N. Dean, A. Simoncig, H. Y. Liu, A. L. Cavalieri, C. Cacho, I. C. E. Turcu, E. Springate, F. Frassetto, L. Poletto, S. S. Dhesi, H. Berger, and A. Cavalleri, Clocking the Melting Transition of Charge and Lattice Order in $1T$ -TaS₂ with Ultrafast Extreme-Ultraviolet Angle-Resolved Photoemission Spectroscopy, *Phys. Rev. Lett.* **107**, 177402 (2011).
- [17] M. Eichberger, H. Schäfer, M. Krumova, M. Beyer, J. Demsar, H. Berger, G. Moriena, G. Sciaini and R. J. D. Miller, Snapshots of cooperative atomic motions in the optical suppression of charge density waves, *Nature (London)* **468**, 799 (2010).
- [18] L. Stojchevska, I. Vaskivskiy, T. Mertelj, P. Kusar, D. Svetin, S. Brazovskii, and D. Mihailovic, Ultrafast switching to a stable hidden quantum state in an electronic crystal, *Science* **344**, 177 (2014).
- [19] C. Sohrt, A. Stange, M. Bauer and K. Rossnagel, How fast can a Peierls-Mott insulator be melted? *Faraday Discuss.* **171**, 243 (2014).
- [20] M. Ligges, I. Avigo, D. Golež, H. U. R. Strand, Y. Beyazit, K. Hanff, F. Diekmann, L. Stojchevska, M. Kalläne, P. Zhou, K. Rossnagel, M. Eckstein, P. Werner, and U. Bovensiepen,

- Ultrafast Doublon Dynamics in Photoexcited $1T$ -TaS₂, *Phys. Rev. Lett.* **120**, 166401 (2018).
- [21] P. Fazekas and E. Tosatti, Charge carrier localization in pure and doped $1T$ -TaS₂, *Physica B+C* **99**, 183 (1980).
- [22] T. Ritschel, H. Berger, and J. Geck, Stacking-driven gap formation in layered $1T$ -TaS₂, *Phys. Rev. B* **98**, 195134 (2018).
- [23] S.-H. Lee, J. S. Goh, and D. Cho, Origin of the Insulating Phase and First-Order Metal-Insulator Transition in $1T$ -TaS₂, *Phys. Rev. Lett.* **122**, 106404 (2019).
- [24] Q. Stahl, M. Kusch, F. Heinsch, G. Garbarino, N. Kretschmar, K. Hanff, K. Rossnagel, J. Geck, and T. Ritschel, Collapse of layer dimerization in the photo-induced hidden state of $1T$ -TaS₂, *Nat. Commun.* **11**, 1247 (2020).
- [25] F. J. Di Salvo, R. G. Maines, J. V. Waszczak, and R. E. Schwall, Preparation and properties of $1T$ -TaSe₂, *Solid State Commun.* **14**, 497 (1974).
- [26] S. Colonna, F. Ronci, A. Cricenti, L. Perfetti, H. Berger, and M. Grioni, Mott Phase at the Surface of $1T$ -TaSe₂ Observed by Scanning Tunneling Microscopy, *Phys. Rev. Lett.* **94**, 036405 (2005).
- [27] S. Colonna, F. Ronci, A. Cricenti, L. Perfetti, H. Berger, and M. Grioni, Scanning Tunneling Microscopy Observation of a Mott-Insulator Phase at the $1T$ -TaSe₂ Surface, *Jpn. J. Appl. Phys.* **45**, 1950 (2006).
- [28] Y. Chen, W. Ruan, M. Wu, S. Tang, H. Ryu, H.-Z. Tsai, R. Lee, S. Kahn, F. Liou, C. Jia, O. R. Albertini, H. Xiong, T. Jia, Z. Liu, J. A. Sobota, A. Y. Liu, J. E. Moore, Z.-X. Shen, S. G. Louie, S.-K. Mo, and M. F. Crommie, Strong correlations and orbital texture in single-layer in $1T$ -TaSe₂, *Nat. Phys.* **16**, 218 (2020).
- [29] X. Shi, W. You, Y. Zhang, Z. Tao, P. M. Oppeneer, X. Wu, R. Thomale, K. Rossnagel, M. Bauer, H. Kapteyn, and M. Murnane, Ultrafast electron calorimetry uncovers a new long-lived metastable state in $1T$ -TaSe₂ mediated by mode-selective phonon coupling, *Sci. Adv.* **5**, eaav4449 (2019).
- [30] F. Boschini, H. Hedayat, C. Dallera, P. Farinello, C. Manzoni, A. Magrez, H. Berger, G. Cerullo, and E. Carpene, An innovative Yb-based ultrafast deep ultraviolet source for time-resolved photoemission experiments, *Rev. Sci. Instrum.* **85**, 123903 (2014).
- [31] C. Manzoni, D. Polli, and G. Cerullo, Two-color pump-probe system broadly tunable over the visible and the near infrared with sub-30 fs temporal resolution, *Rev. Sci. Instrum.* **77**, 023103 (2006).
- [32] See Supplemental Material at <http://link.aps.org/supplemental/10.1103/PhysRevB.102.161105> for details of crystal growth, electronic transport measurements, Raman spectroscopy, full-wave-vector ARPES, LEED, and further analysis of TR-ARPES data.
- [33] M. Bovet, D. Popovi, F. Clerc, C. Koitzsch, U. Probst, E. Bucher, H. Berger, D. Naumovi, and P. Aebi, Pseudogapped Fermi surfaces of $1T$ -TaS₂ and $1T$ -TaSe₂: A charge density wave effect, *Phys. Rev. B* **69**, 125117 (2004).
- [34] F. Clerc, M. Bovet, H. Berger, L. Despont, C. Koitzsch, O. Gallus, L. Patthey, M. Shi, J. Krempasky, M. G. Garnier, and P. Aebi, Spin-orbit splitting in the valence bands of $1T$ -TaS₂ and $1T$ -TaSe₂, *J. Phys.: Condens. Matter* **16**, 3271 (2004).
- [35] P. Aebi, T. Pillo, H. Berger and F. Lévy, On the search for Fermi surface nesting in quasi-2D materials, *J. Electron. Spectrosc. Relat. Phenom.* **117**, 433 (2001).
- [36] P. Knowles, B. Yang, T. Muramatsu, O. Moulding, J. Buhot, C. J. Sayers, E. Da Como, and S. Friedemann, Fermi Surface Reconstruction and Electron Dynamics at the Charge-Density-Wave Transition in TiSe₂, *Phys. Rev. Lett.* **124**, 167602 (2020).
- [37] M. P. Seah and W. A. Dench, Quantitative electron spectroscopy of surfaces: A standard data base for electron inelastic mean free paths in solids, *Surf. Interface Anal.* **1**, 2 (1979).
- [38] S. Ji, O. Grånäs, K. Rossnagel, and J. Weissenrieder, Transient three-dimensional structural dynamics in $1T$ -TaSe₂, *Phys. Rev. B* **101**, 094303 (2020).
- [39] J. Demsar, L. Forro, H. Berger and D. Mihailovic, Femtosecond snapshots of gap-forming charge-density-wave correlations in quasi-two-dimensional dichalcogenides $1T$ -TaS₂ and $2H$ -TaSe₂, *Phys. Rev. B* **66**, 041101(R) (2002).
- [40] J. E. Smith, Jr., J. C. Tsang, and M. W. Shafer, Raman spectra of several layer compounds with charge density waves, *Solid State Commun.* **19**, 283 (1976).
- [41] J. C. Tsang, J. E. Smith, Jr., M. Shafer, and S. F. Meyer, Raman spectroscopy of the charge-density-wave state in $1T$ - and $2H$ -TaSe₂, *Phys. Rev. B* **16**, 4239 (1977).
- [42] S. Uchida and S. Sugai, Infrared and Raman studies on commensurate CDW states in transition metal dichalcogenides, *Physica B+C* **105**, 393 (1981).
- [43] S. Sugai, K. Murase, S. Uchida, and S. Tanaka, Comparison of the soft modes in tantalum dichalcogenides, *Physica B+C* **105**, 405 (1981).